Published in final edited form as:
J Immunol. 2014 March 15; 192(6): 2812–2820. doi:10.4049/jimmunol.1301794.

Mouse Mast Cell Protease 4 and 5 Mediate Epidermal Injury Through Disruption of Tight Junctions

Lora G. Bankova[*], **Cecilia Lezcano**[†], **Gunnar Pejler**[‡], **Richard L. Stevens**[*], **George F. Murphy**[†], **K. Frank Austen**[*], and **Michael F. Gurish**[*]

[*]Division of Rheumatology, Immunology and Allergy, Brigham and Women's Hospital, Harvard Medical School, Boston, MA 02115

[†]Department of Pathology, Brigham and Women's Hospital, Harvard Medical School, Boston, MA 02115

[‡]Department of Anatomy, Physiology and Biochemistry, Swedish University of Agricultural Sciences, Uppsala, Sweden

Abstract

We previously established a mast cell (MC)-dependent thermal injury model in mice with ulceration and scar formation that depended on non-redundant functions of mouse MC protease 4 (mMCP4) and mMCP5. We hypothesized that MC activation is an early event and now find by histology that exocytosis of granule contents occurred by 2 min after thermal injury in wild type (WT) C57BL/6 mice and in the mMCP4- or mMCP5-deficient mice. The degranulation was equivalent for MCs in the dermis and hypodermis of all three strains, but only the WT mice showed an appreciable increase in epidermal thickness. There was no loss of total MCs, partially degranulated plus intact, over the 4 h of observation. By electron microscopy, MCs in all strains showed early zonal degranulation at 30 s with marked progression in magnitude by 120 s and no mitochondrial injury or cellular necrosis. Concomitantly there was an increase in intercellular spaces indicative of tight junction (TJ) disruption in WT mice but not in the mMCP4- or mMCP5-deficient strains. The desmosomes were intact in all strains. Immunodetection of the TJ protein claudin 4 in WT and mMCP5-deficient mice indicated a significant reduction after scald injury while mMCP4$^{-/-}$ mice showed no significant changes. Taken together, these findings reveal that a second degree burn injury can initiate an immediate novel zonal degranulation of MCs throughout all skin layers and a disruption of the epidermal TJs dependent on the non-redundant presence of mMCP4 and mMCP5.

Introduction

In mice, thermal injury characteristic of a second-degree burn is followed in 3 d by ulceration and subsequent skin remodeling with scar formation (1). However, mice deficient in the complement pathway or a natural IgM specific for non-muscle myosin heavy chain are protected from this progression. The administration of a blocking peptide of the natural IgM immediately after the thermal trauma is also fully protective suggesting that the model reflects an inflammatory process that can be contained to eliminate progression of the injury (1–3). We found that MC-deficient mice of the WBB6F1/J-Kit^{W}/Kit$^{W\text{-}v}$ strain and strains

Address correspondence and reprint request to Dr. Michael F. Gurish, Division of Rheumatology, Immunology and Allergy, Brigham and Women's Hospital, Smith Research Building, Room 616, One Jimmy Fund Way, Boston, MA 02115. Phone: 617-525-1235, FAX: 617-525-1310, mgurish@partners.org.

Disclosures
The authors have no conflicts of interest to declare.

lacking secretory granule proteases mMCP4, a chymase, and mMCP5, an elastase, but not several others were also protected (4). Topical application of human MC chymase (the human homolog of mMCP4) to the injury site in the mMCP4-deficient strain within the first hour abrogated the protection while its application to the thermally challenged site in the mMCP5-deficient mice had no effect. Conversely, topical application of recombinant mMCP5 or human neutrophil (PMN) elastase to the mMCP5-deficient strain abrogated the protection but only in this strain. With abrogation of protection, the injury site of each deficient strain progressed to ulceration by d 3 and scar formation by d 11–12 just as in WT mice (4).

We speculated that the degranulation of MCs to release the proteases involved in thermal injury would be earlier than the 2 h time point at which we had previously assessed for degranulation (4). Indeed, we now find near maximal degranulation at 2 min, the earliest time point examined by histology. Turning to electron microscopy (EM), we see zonal degranulation at 30 s with progression to near complete degranulation at 120 s suggesting a secretory process. Degranulating MCs consistently contained intact mitochondria and were devoid of other indications of necrosis or apoptosis. The MC degranulation in WT mice is followed by disruption of the TJs detected at 120 s without injury to the desmosomes. The two protease deficient strains showed zonal degranulation at 30 s with progression at 120 s but no disruption of the TJs. As assessed by immunohistochemistry at 2 min, the TJ protein claudin 4 was significantly decreased in WT and mMCP5-deficient mice but not in mMCP4-deficient mice suggesting a possible basis for protection in the latter strain.

Materials and Methods

Animals

WT C57BL/6 mice were obtained from Taconic Laboratories (Germantown, NY). The mice deficient in mMCP4, N7 (5) and mMCP5, N10 (6) were on a C57BL/6 mouse genetic background. These protease-deficient strains were maintained in specific pathogen-free colonies at the Dana Farber Cancer Institute (Boston, MA). The use of mice for these studies was in accordance with institutional guidelines with review and approval by the Animal Care and Use Committee of the Dana Farber Cancer Institute.

Reagents

Rabbit polyclonal Abs for immunostaining of TJ claudins 1, 3, and 4 and occludin as well as an isotype control were obtained from Invitrogen (Camarillo, CA). Protein Block Serum-free and Dual Endogenous Enzyme Block were obtained from DakoCytomation (Carpintera, CA). For epitope retrieval, EDTA solution pH 8.0 was obtained from Invitrogen (Camarillo, CA). Goat anti-rabbit biotinylated secondary Ab and Vectastain ABC alkaline phosphatase kit were obtained from Vector Laboratories (Burlingame, CA). Sigma*FAST* Fast Red TR/Naphthol was obtained from Sigma-Aldrich (St Louis, MO). Hoechst 33342 fluorescent stain was obtained from Thermo Scientific (Rockford, IL). Purified human neutrophil elastase was obtained from Enzo Life Sciences (Farmingdale, NY).

Epidermal scald procedure

The epidermal scald procedure was performed as previously described (4). All mice ranged between 8 and 14 wks of age. A rectangular area on the back was clipped and shaved 24 h prior to the thermal challenge procedure. For the thermal challenge, mice were anesthetized with an i.p. injection of ketamine (10 mg/kg) and xylazine (20 mg/kg) for full sedation. A template created from a high-impact nonheat-conducting plastic container, was used to produce a square-shaped 1 cm^2 exposure site on the interscapular dorsum area (~2.5% of the body surface area). With the template held in position, the shaved skin was scalded in a

circulating water bath at 54°C for 30 s. Two different controls were used for the experiments. The first set of controls was mice that underwent back skin hair removal and anesthesia and were placed in the plastic container but not submerged in the water bath (indicated as “no scald”). A second set of control samples came from an area of unsubmerged back skin distant from the scalded site (outside the scald area). For the post burn cooling experiments, mice were initially submerged in a circulating water bath as above for 30 s and immediately transferred in the same device to room temperature or to an ice bath with a temperature of 1°C for 60 s or for 30 s followed by room temperature. Control mice were submerged in an ice bath for 60 s. All mice were sacrificed 1 min after their scald. For elastase reconstitution experiments, mMCP5-deficient and WT mice were scalded as above. Immediately after the scald, a 1 cm^2 piece of gauze saturated with 100 μl of elastase solution (2.5 μg elastase/100 μl HBSS) or HBSS was applied to the scald site of each mouse strain. The gauze was kept in place for 10 min after scalding at which point the mice were sacrificed.

Histology and quantitative assessment of injury

Skin was harvested from the prepared dorsal sites at multiple time points after the scalding procedure in different cohorts of mice – 30 s, 2 min, 10 min, 1 h, 2 h and 4 h. The tissue was fixed in 4% paraformaldehyde in PBS for 18 h, changed to PBS, and kept at 4°C. For histochemical evaluation, the tissues were embedded in glycolmethacrylate. Tissue sections, 2.5 μm thick, were assessed by their chloroacetate esterase (CAE) reactivity for quantitation of the number of MCs and PMNs and were counterstained with hematoxylin for general morphologic examination (7). Total MCs and PMNs were quantitated in 9 unit areas (UA) (1 UA = 1.2 × 0.9 mm = 1.08 mm^2) at low power to calculate their value (per 9 UA) for each individual animal. MCs were examined for degranulation under high power (400× or 630×). A MC was determined to be degranulating when three or more granule cores were found outside of the cell (6). A small fraction of MCs with loss of some intracellular granules were detectable by CAE histochemistry even without associated extracellular granule cores and considered to be degranulated. However, the majority of MCs without extracellular granules retained tightly packed intracellular granules, and were considered non-degranulating and intact. The numbers of the degranulating and intact MCs at each time point were added to provide the total number of MCs at the skin site. Digital photographs of the thermally challenged area were taken at 100× magnification (low-power field, LPF), and the epidermal area was evaluated using Image J software (National Institutes of Health, Bethesda, MD). The epidermal edema was determined by measuring the area of epidermis (expressed in square micrometers, μm^2) of at least 3 photographs representative of 3 separate sites of the thermally challenged area and expressed as the average of the 3 measurements. Spongiosis was defined as evidence of epidermal intercellular edema, resulting in widened intercellular spaces (8). Acantholysis was defined as dissolution of intercellular junctions resulting in rounded, detached keratinocytes (8).

For immunohistochemistry and fluorescence, tissues were embedded in paraffin and tissue sections (5 μm) were stained with polyclonal rabbit anti-mouse Abs against claudins 1, 3, and 4 or occludin or mMCP4 (9) and a rabbit polyclonal IgG negative control. For target retrieval, slides were immersed in 1× EDTA solution, pH 8.0 at 95°C for 10 min. Endogenous alkaline phosphatase activity was inhibited with the Dual Endogenous Enzyme Block. Non-specific binding was eliminated using the Protein Block Serum-Free. Samples were incubated overnight at 4°C, with primary Abs titered to the lowest concentration that produced immunoreactivity in control samples. After labeling with a biotinylated secondary goat anti-rabbit Ab, immunodetection was performed using the avidin-biotin-phosphatase complex with Sigma*FAST* Fast Red TR/Naphthol as the phosphatase substrate. Nuclear staining for the fluorescence samples was performed with Hoechst 33342 nuclear stain. We

used the fluorescence property of Fast Red to visualize the positive stain with fluorescence microscopy (excitation 568 nm, detection using Texas Red filter) (10) using a Nikon E800 equipped with an eyepiece and a 20× objective and Spot Slider RT-3 camera (Diagnostic Instruments, Sterling Heights, Michigan). Images were overlaid using ImageMagick (ImageMagick Studio LLC, open source software). The area of epidermis was selected on overlaid pictures including nuclear stain and TJ fluorescent stain. Each selection was then superimposed on the grey scale picture for claudin 4. Measurement of the fluorescence intensity (mean of three separate areas) was expressed as number of pixels per μm^2 using Image J software.

Electron microscopy

For EM, all biopsies were immersed 30 s or 120 s after thermal injury in Karnovsky's II fixative, finely sectioned, fixed overnight and rinsed in 0.1 M sodium cacodylate buffer (pH 7.4). Then the tissues were fixed in 1% osmium tetroxide in 0.1 M cacodylate buffer, dehydrated in graded ethanol solutions, and embedded in Epon. One μm thick sections were prepared with a microtome and stained with toluidine blue for light microscopic identification of MCs. Fields demonstrating MCs were identified and blocks were further trimmed in preparation for ultramicrotomy. Ultrathin sections (0.87 nm) were prepared from selected fields, stained with uranyl acetate and lead citrate, and examined with a JEOL JEM-1010 electron microscope over a direct magnification range of 3000 to 80000×.

Statistical analysis

For comparisons between two time points, Mann-Whitney non-parametric tests were performed. Changes in claudin 4 immunodetection over time were measured and compared between the different strains with a two-way ANOVA test. P values less than 0.05 were considered statistically significant and the following designations used: *, $p < 0.05$; **, $p < 0.01$; ***, $p < 0.001$. In samples with only 2 replicates, we report mean ± ½ range. Statistical analysis was performed with Prism software (GraphPad Software, Inc., San Diego, CA).

Results

MC degranulation is an immediate response to thermal challenge to skin in WT mice

The time course of thermal injury-induced MC degranulation in C57BL/6 WT mice was initially assessed by histology (Fig. 1A) and then re-examined at the earliest intervals by EM. Two minutes after thermal injury, 38 ± 5% of the MCs in the skin of WT mice at the challenged site had degranulated based on the presence of abundant extracellular CAE+ granule cores (Fig. 1B). In contrast, the MCs in WT mice subjected only to hair removal and anesthesia in parallel were only 7 ± 1% degranulated. The percent of MCs showing degranulation with thermal challenge to skin did not change significantly in a time course of up to 4 h after exposure (38 ± 5% at 2 min, 44 ± 4% at 10 min, 46 ± 3% at 1 h, 39 ± 4% at 2 h and 39 ± 5% at 4 h). Correspondingly, there was a decrease in the number of intact MCs from 102 ± 8 per LPF with no scald, to 64 ± 6 at 2 min, 67 ± 5 at 10 min, 57 ± 4 at 1 h, 57 ± 5 at 2 h, and 54 ± 1 at 4 h post scald (Supplemental Fig. 1A). The total number of intact and degranulated MCs at the challenge site did not change over this time course (Supplemental Fig. 1B). No differences were found in the percent of degranulating MCs in the papillary dermis, reticular dermis, or hypodermis (Supplemental Fig. 1C). Approximately half of the MCs were in the reticular dermis with the rest distributed between papillary dermis and hypodermis as previously reported (4) (Supplemental Fig. 1D). Margination of PMN within the vasculature of the dermis and hypodermis, noted at 2 min, increased at 1 h, the time point at which extravasation was significant (Fig. 1D, E)

To demonstrate that the extent of MC degranulation in the scald site at 30 s could be attenuated, after a scald we immediately transferred one cohort to room temperature and two cohorts of the mice to an ice bath for 30 and 60 s, respectively. While the cohort transferred to room temperature for 60 s had degranulation of 47% of the MC in full skin at the burn site, the cohort subjected to immediate cooling for 30 s had significantly reduced degranulation of 20% (Supplemental Fig. 2). Cooling for 60 s had no further effect (21% degranulation). Thus, the interval for achieving inhibition of MC degranulation by cooling was 30 s or less. The degranulation associated with cooling alone without a scald was about 7% and above background.

By EM, MC activation was detectable by granule changes as early as 30 s after thermal trauma. There was enlargement of some granules with merging of granule membranes and "solubilization" of granule contents that appeared as flocculent, electron-lucent material while other granules remained electron dense and unaltered (Fig. 1C, *top panel, blue and red arrows*). The changes in granule ultrastructure were not uniform and frequently affected only a group of granules at one pole of a given cell. Notably, the mitochondria of the MCs were intact. By 120 s, MC degranulation was generally more uniform throughout the cell (Fig. 1C, *bottom panel*) although there were occasional cells wherein some granules remained electron dense and unaltered. In contrast, the MCs in an area of skin distal from the challenge site (outside scald) contained electron dense granules throughout the cytosol without evidence of swelling, merging of granule membranes, or solubilization of granule contents (Fig. 1C, *top panel, insert*).

Disruption of TJs is a very early epidermal response to thermal injury of skin in WT mice

As assessed by routine histology, there was a significant increase in the epidermal area suggestive of edema at 2 min, which increased further at 10 min and 1 h after the thermal challenge (Fig. 2A, B). The mean histologically determined epidermal area in shaved skin of WT mice not subjected to scalding was 23589 ± 677 μm^2 (Fig. 2B). In shaved skin of mice subjected to a scald burn the epidermal area increased to 27935 ± 1784 μm^2 at 2 min, 30293 ± 1212 μm^2 at 10 min, and 30358 ± 771 μm^2 at 1 h. No epidermal edema was detected in skin biopsies taken from the skin site outside the scald area (mean epidermal area 23988 ± 37μm^2, n=2). Areas of spongiosis were noticeable 10 min and 1 h after injury (Fig. 2A, *black arrows*). No acantholysis was observed at any of the time points evaluated (2 min, 10 min, and 1 h).

Samples for EM obtained 30 s and 120 s after thermal challenge were taken close to a degranulating MC and processed as thin sections. The two main components of the intercellular junction machinery are desmosomes and TJs. The TJs are composed of thin bands of plasma membrane proteins that completely encircle a polarized cell and are in contact with similar thin bands on adjacent cells. TJs cannot be identified by conventional microscopy. However, when thin sections are viewed by EM, the plasma membranes of adjacent cells appear at intervals to touch each other, forming points of contact between the two cells where the two plasma membranes appear indistinct or even to fuse (11). Skin biopsies from an area outside the scald site showed intact keratinocytes and normal interepithelial TJs (data not shown). Thirty seconds after thermal injury, no distinct changes were observed in the TJs of the epidermis (Fig. 2C, *circle*) or in the desmosomes (Fig. 2C, *arrow*). However, 2 min after thermal trauma, there was loss of integrity of the TJs characterized by focal widening of the spaces separating the adjacent keratinocyte plasma membranes (Fig. 2D, E, *circles*). In contrast, nearby desmosomes appeared normal in structure and number at this time point (Fig. 2D, E, *arrows*), and no other ultrastructural alterations were seen except for MC degranulation. These EM findings were consistent in 2 separate experiments with a total of 8 mice.

Immunodetection of the TJ protein claudin 4 diminishes after thermal injury

The EM findings that TJs are differentially affected relative to desmosomes in a scald burn injury model prompted an examination of the status of TJ proteins typically expressed in the epidermis. As assessed immunohistochemically with detection by fluorescence, there was decreased claudin 4 in the epidermis of WT mice in the first 2 min following scalding (Fig. 3A). Quantitation of claudin 4 immunodetection revealed a significant reduction from 42 ± 4 pixels/μm^2 at baseline to 19 ± 2 pixels/μm^2 at 2 min with no further reduction after that time point (21 ± 2 at 10 min and 22 ± 2 at 1 h after injury) (Fig. 3B). In contrast, there was no change in the immunodetectable levels of the TJ proteins claudin 1 (the main structural protein of epidermal TJs), claudin 3 or occludin (data not shown). The amino acid sequence of mouse claudin 4 (12) is 45% and 70% identical to claudin 1 (13) and 3 (12), respectively, indicating that the loss of claudin 4 is selective.

Thermal injury in mMCP4-deficient mice induces MC degranulation without epidermal injury

In an initial approach to exclude a gross defect in MC degranulation kinetics or percent involvement in the mutant strain, we examined MC degranulation in mMCP4$^{-/-}$ mice at 2 min, 10 min and 60 min post thermal challenge. The morphology of the mMCP4$^{-/-}$ MCs is somewhat different from WT controls as they are smaller in size and their granules stained less intensely red with CAE. Nonetheless, MC granules are readily visible in the cytoplasm of non-challenged mice and the percent degranulation of skin MCs with thermal challenge is comparable to that of WT mice (Fig. 4A, B). The total number of MCs at baseline per assay site was 111 ± 10 in WT mice and 64 ± 10 in the mMCP4$^{-/-}$ mice. EM confirmed that zonal MC degranulation similar to that seen in WT animals is present at 30 s (Fig. 4C, *top panel, red arrow*). As observed in WT mice, the secretory degranulation in MC from the mMCP4$^{-/-}$ strain progresses to involve more granules at 120 s (Fig. 4C, *bottom panel*). The insert shows a MC with uniform electron dense granules from an unscalded site. There was a trend toward an increase in PMN margination in the mMCP4$^{-/-}$ as compared to the WT mice at the 2 min time point (p=0.0745). No differences in PMN margination or extravasation were noted at the subsequent time points (Fig. 4D, E).

There was no epidermal edema after thermal challenge of the mMCP4-deficient strain (Fig. 5A, B) and spongiosis was minimal when present. As in the WT mice no acantholysis was apparent in the epidermis. By EM, there was no disruption of the TJs (*circles*) between cells in thin sections at 30 s or 120 s and the desmosomes (*arrows*) were intact (Fig. 5C–E). Furthermore, in contrast to the significant reduction in immunodetection of claudin 4 in WT mice after the scald, the change in the level of claudin 4 was not significant at 2, 10, or 60 min (Fig. 6A, B) in the mMCP4-deficient strain examined in parallel. Mice lacking mMCP4 were noted to have a lower baseline level of claudin 4. Other TJ proteins examined including claudin 1, claudin 3, and occludin were detected at similar levels as in the WT controls and did not change after thermal challenge (data not shown).

The epidermal protection in the mMCP4$^{-/-}$ mice suggested that this protease may be directly acting on the TJs of the keratinocytes. In reexamining WT mice, we noted that extruded granule cores detected by the enzymatic activity of mMCPs (CAE reactivity, Fig. 1A) remained relatively close by the parent cell. We observed no mMCP4 in the epidermis by histochemistry or immunostaining (data not shown) including areas of the epidermis with spongiosis. We did not find any topological association between the histological changes occurring in the epidermis and the histological detection of proteases or immunodetection of mMCP4 in the dermis (Fig. 2A, *arrows*).

Thermal injury in mMCP5-deficient mice induces degranulation with mild epidermal changes

MCs of the mMCP5$^{-/-}$ mouse were smaller than those of WT mice. Nonetheless, intracellular granules and extracellular granule cores were easily detectable by CAE reactivity using a higher magnification (630×) (Fig. 7A). The percent degranulation of mMCP5$^{-/-}$ mice was comparable to WT mice at 2, 10, and 60 min (Fig. 7B). EM showed that the degranulation of MCs in the mMCP5$^{-/-}$ mice is present with a zonal presentation at 30 s post challenge (not shown) and that there is progression of the secretory granule changes at 120 s (Fig. 7C and *insert*). No differences in the PMN response were noted as PMN margination in the vasculature and their extravasation in the mMCP5-deficient mice was similar to that of WT mice (Fig. 7D, E).

After thermal challenge, there was a mild increase of the epidermal area suggestive of slight edema at the early time points of 2 min and 10 min with resolution by 1 h by histology (Fig. 8A, B). Spongiosis was detectable in a few areas. No acantholysis was apparent in the epidermis. By EM, at the 120 s time point, the TJs (*circles*) were intact as were the desmosomes (*arrows*) (Fig. 8C, D). Reconstitution of the missing protease activity by application of human elastase to mMCP5$^{-/-}$ mice immediately after scalding led to epidermal edema similar in degree to that observed in WT mice assessed at 10 min post scald (Fig. 8E). Application of elastase to WT mice after scalding did not further augment the epidermal edema (Fig. 8E). By immunostaining there was a decrement in claudin 4 protein that was similar to that observed in WT mice (Fig. 9A, B). Other TJ proteins examined including claudin 1, claudin 3, and occludin were detected at similar levels as the WT controls and did not change after thermal challenge (data not shown).

Discussion

We have shown for the first time to our knowledge that MC degranulation is a virtually immediate response to second-degree thermal trauma in the C57BL/6 mouse. MC degranulation detected by EM occurs within 30 s after the thermal insult, a time point at which epidermal changes are not seen. The initial zonal degranulation at 30 s progresses to involve many more cytoplasmic granules by 120 s with fusion of granule membranes and loss of electron density compatible with a secretory process. The integrity of the mitochondria in the MCs also favors such a view. By histologic assessment, the percent of degranulated MCs reached a peak at 120 s and did not increase over the subsequent 4 h. The lack of decline in the total number of MCs, degranulated and intact, at a thermal injury site over 4 h is additional evidence for a non-cytotoxic secretory MC response. The further finding by histology that the percent of degranulating MCs is similar in the compartments underlying the epidermis, namely the papillary and reticular dermis and hypodermis, suggests that the thermal trauma-induced signal is almost immediately distributed to deeper tissue. The finding that immediate cooling of the skin burn site significantly prevented degranulation of more than one half of the MC could be due to inhibition of complement activation, a direct effect on MC exocytosis or both, and supports the finding that an initial phase of the trauma-elicited response is inflammatory and can be attenuated.

The delay of detectable ultrastructural disruption of epidermal TJs to 120 s in WT mice when MC degranulation is already substantial and the absence of TJ disruption in the mMCP4- and mMCP5-deficient strains implies a role for these proteases in the epidermal changes. The absence of ultrastructurally detectable injury to the desmosomes and the specific change in immunodetection of only one of the TJ proteins – claudin 4, suggests that the tissue changes are an indirect effect of the scald mediated by a MC response that is secretory and not cytotoxic. The plateau of MC degranulation at 120 s by histology occurs before influx of PMNs or any other inflammatory cell type implying that PMN-derived

enzymes are not causing these discrete initial changes in the epidermis. However, the trend toward increased PMN margination and extravasation noted in the mMCP4−/− mice at 2 min suggests that this chymase may provide a regulatory role in this response as observed for alarmins in other models (14). In the context of our previous findings that topical application of the missing MC protease function to the scald site leads to ulceration and scaring in the otherwise protected deficient strains (4), the new data suggest that MC activation and consequent specific disruption of TJs are initial events in thermal injury that provides both a signal and a susceptible microenvironment. These MC proteases have no effect when applied directly to shaved unscalded skin (4). Although the edema during the initial 1 h post burn was limited to the epidermis, the tissue injury progresses to ulceration, loss of hair follicles and denaturation of collagen in the dermis as the inflammatory process that is set off by the thermal trauma unfolds (4).

An interesting feature of the degranulating MCs is the “zonal” character at 30 s with both activated and intact secretory granules residing in the same cell, a profile seen previously in dermatographism, a form of physical urticaria in humans (15). The nature of the degranulation, starting at one pole of the cell may reflect some polarization in the delivery of the injury signal. The inflammatory pathway leading to ulceration depends on a natural IgM directed against non-muscle myosin heavy chain, the complement cascade and MCs (1–4, 6, 16). Although the current study reveals a very early role for the MC and two of its secretory granule proteases in an inflammatory process that amplifies thermal injury, we do not know what activates the MCs so quickly. Reminiscent of the reduced degranulation with tissue cooling, an increase in post burn tissue temperature may facilitate an induced physiologic degranulation. In addition, a polarized expression of the non-muscle myosin heavy chain Ag and or a lectin-dependent activation of complement at the burn site are candidates for initiation. A neurogenic signal also has merit based on the association of MCs with nerves in peripheral tissues (17) and the comparable degranulation in both dermis and hypodermis.

Two of the major components of epithelial barriers are the desmosomes, which provide the physical bonds between cells, and the TJs, which regulate the selective permeability to water and electrolytes (18). The epidermis has an additional cornified layer of anuclear cells embedded in a matrix of extracellular lipids and structural proteins making the epidermal barrier difficult to breach (19). TJ integrity and distribution is altered in several skin diseases, most notably atopic dermatitis (20) and psoriasis (21). A direct role for MCs or MC proteases in regulation of TJs in the skin has not been reported so far. However, the intestinal epithelium with its single layer of cells provides a direct model for studies of intercellular junction integrity and transepithelial permeability and several reports point to a role of MCs and MC secretory granule proteases in the control of both homeostatic epithelial permeability and permeability alterations in pathologic states. In naïve mice, regulation of intestinal transepithelial permeability by MCs was implied by the decrease in this function in the MC-deficient $Kit^{W\text{-}sh}$ strain on a C57BL/6 background (22). Naïve mMCP4$^{-/-}$ mice also had decreased permeability for FITC dextran and this epithelial abnormality was corrected by adoptive transfer of WT but not mMCP4$^{-/-}$ bone marrow-derived immature MCs. In addition, application of human MC chymase to an epithelial monolayer in an Ussing chamber increased transepithelial permeability within 30 min of application, the first time point reported. The epithelial permeability defect in the intestine of mMCP4$^{-/-}$ mice was linked to dysregulated expression of the major intestinal TJ protein claudin 3 (22). We found a lower baseline level of immunodetectable claudin 4, one of the major TJ proteins in the skin, in mMCP4-deficient mice but no change after thermal challenge in this strain. The decrement in claudin 4 immunodetection in the skin of WT mice with thermal challenge could be a direct effect of the chymase or an indirect consequence via activation of matrix metalloproteases (23).

We could not detect any mMCP4 by its enzymatic activity as an esterase or by immunodetection in the scalded epidermis even in areas showing spongiosis (data not shown). This is in keeping with previous studies showing that the highly positively charged proteases such as mMCP4, 5 and 6 utilize arginine and lysine residues to remain associated with the highly negatively charged serglycin proteoglycans even after release into the extracellular milieu and despite the change in pH from about 5 to 7 (24–26). The functions of the highly cationic proteases such as chymase are enhanced by their association with heparin proteoglycans (27, 28). Nonetheless, it is conceivable that scalding, by virtue of an increase in tissue temperature, facilitates dissociation of the mMCP4 from the proteoglycan-protease complex and or diffusion to act directly in the epidermis. In any case, the integrated burn model involves changes in two tissues, degranulation of MCs in the dermis and hypodermis beginning at 30 s and burn site restricted disruption of epidermal junctions with loss of immunodetection of the intracellular C-terminus of claudin 4 at 120 s. The pathway leading to the disruption of the epidermal TJ and the inflammation that is rapidly activated by the combination of thermal trauma and the release of the chymase, is absolutely dependent on this enzymatic activity as evidenced by the reconstitution of the full course of the injury in mMCP4$^{-/-}$ mice treated with human MC chymase but not elastase, during the first hour post scald (4).

An epidermal desmosome target for mMCP4 has recently been identified in a mouse model of bullous pemphigoid, an autoimmune disease in which MCs were found to degranulate in the bullous lesions (29, 30). The bullae formation is dependent on the presence of an Ab against the epidermal hemidesmosome transmembrane protein BP180. Prolonged exposure (12 h) of neonatal mouse skin explants to a high concentration (1 μg/ml) of mMCP4-induced cleavage of the hemidesmosome protein BP180 (30). However, we detected no changes in the hemidesmosomes by EM after thermal trauma at the very early time points we examined to assess for onset of MC degranulation and cleavage of TJs.

Mice lacking mMCP5 also are protected from the inflammation and downstream scarring that occurs after MC dependent second-degree thermal injury (4). There was no impairment of MC degranulation assessed by histology and EM. The skin exhibited a transient mild epidermal edema by histology at 2 and 10 min but no loss of TJ integrity was detected by EM at 120 s. We were able to restore full epidermal edema in mMCP5$^{-/-}$ mice by reconstituting the missing protease activity immediately following scalding consistent with our previous findings that application of elastase restores ulceration in the elastase-deficient mice (4). Of additional note, the epidermal edema at the burn site in WT mice was not increased by the topical application of elastase. Thus, the topical elastase was redundant for epidermal edema in the burn site of WT mice yet critical to a full response in the mMCP5-deficient mice. Claudin 4 was decreased by immunodetection in mMCP5$^{-/-}$ mice similarly to the findings in WT mice suggesting that the protective effect of this protease deficiency is not directed to this TJ protein. This difference from mMCP4 null mice is consistent with our previous findings that topical application to generate full burn injury in the respective deficient strain required applying the particular activity of the missing protease (4). There is a slight attenuation of neutrophil extravasation in mMCP5$^{-/-}$ mice, which might be able to supply the missing elastolytic activity, but the difference did not reach significance.

In summary, we show that thermal challenge sufficient for a second-degree burn to the skin causes immediate non-cytotoxic MC zonal degranulation at 30 s with expansion of this secretory process at 120 s. That MC activation in the dermis and hypodermis precedes the disruption of the TJs suggests an initiating role for the MC in the early loss of claudin 4 and appearance of epidermal edema. This sequence is supported by the protection of the TJs in the protease deficient strains, which undergo immediate degranulation comparable to the WT strain with thermal challenge.

Supplementary Material

Refer to Web version on PubMed Central for supplementary material.

Acknowledgments

We wish to thank Dr. Juying Lai for the excellent technical assistance in performing all of the histochemical staining. We also wish to acknowledge the use of the Boston Children's Hospital Intellectual and Developmental Disabilities Research Center Cellular Imaging Core. Finally, we wish to thank Dr. Edward Brignole for his assistance with image analysis.

This work was supported by grants from the National Institutes of Health: P50-GM52585, R01-AI083516, P30-HD18655 and T32-AI007306, and the Joycelyn C. Austen Fund for Career Development of Women Physician Scientists.

References

1. Suber F, Carroll MC, Moore FD Jr. Innate response to self-antigen significantly exacerbates burn wound depth. Proc. Natl. Acad. Sci. U S A. 2007; 104:3973–3977. [PubMed: 17360462]
2. Haas MS, Alicot EM, Schuerpf F, Chiu I, Li J, Moore FD, Carroll MC. Blockade of self-reactive IgM significantly reduces injury in a murine model of acute myocardial infarction. Cardiovasc. Res. 2010; 87:618–627. [PubMed: 20462867]
3. Zhang M, Austen WG Jr, Chiu I, Alicot EM, Hung R, Ma M, Verna N, Xu M, Hechtman HB, Moore FD Jr, Carroll MC. Identification of a specific self-reactive IgM antibody that initiates intestinal ischemia/reperfusion injury. Proc. Natl. Acad. Sci. U S A. 2004; 101:3886–3891. [PubMed: 14999103]
4. Younan G, Suber F, Xing W, Shi T, Kunori Y, Abrink M, Pejler G, Schlenner SM, Rodewald HR, Moore FD Jr, Stevens RL, Adachi R, Austen KF, Gurish MF. The inflammatory response after an epidermal burn depends on the activities of mouse mast cell proteases 4 and 5. J. Immunol. 2010; 185:7681–7690. [PubMed: 21076070]
5. Tchougounova E, Pejler G, Abrink M. The chymase, mouse mast cell protease 4, constitutes the major chymotrypsin-like activity in peritoneum and ear tissue. A role for mouse mast cell protease 4 in thrombin regulation and fibronectin turnover. J. Exp. Med. 2003; 198:423–431. [PubMed: 12900518]
6. Abonia JP, Friend DS, Austen WG Jr, Moore FD Jr, Carroll MC, Chan R, Afnan J, Humbles A, Gerard C, Knight P, Kanaoka Y, Yasuda S, Morokawa N, Austen KF, Stevens RL, Gurish MF. Mast cell protease 5 mediates ischemia-reperfusion injury of mouse skeletal muscle. J. Immunol. 2005; 174:7285–7291. [PubMed: 15905575]
7. Friend DS, Ghildyal N, Austen KF, Gurish MF, Matsumoto R, Stevens RL. Mast cells that reside at different locations in the jejunum of mice infected with Trichinella spiralis exhibit sequential changes in their granule ultrastructure and chymase phenotype. J. Cell. Biol. 1996; 135:279–290. [PubMed: 8858180]
8. Murphy, GF. Structure, Function and Reaction Patterns. In: Murphy, GF., editor. Dermatopathology : a practical guide to common disorders. Philadelphia, PA: W.B Saunders; 1995. p. 3-45.
9. Forsberg E, Pejler G, Ringvall M, Lunderius C, Tomasini-Johansson B, Kusche-Gullberg M, Eriksson I, Ledin J, Hellman L, Kjellen L. Abnormal mast cells in mice deficient in a heparin-synthesizing enzyme. Nature. 1999; 400:773–776. [PubMed: 10466727]
10. Speel EJ, Schutte B, Wiegant J, Ramaekers FC, Hopman AH. A novel fluorescence detection method for in situ hybridization, based on the alkaline phosphatase-fast red reaction. J. Histochem. Cytochem. 1992; 40:1299–1308. [PubMed: 1506667]
11. Lodish, HF. Integrating cells into tissues. In: Lodish, HF.; Berk, A.; Matsudaria, P.; Kaiser, CA.; Krieger, M.; Scott, MP.; Zipursky, SL.; Darnell, J., editors. Molecular cell biology. 5th ed.. New York, NY: Scientific American Books : Distributed by W.H. Freeman; 2004. p. 197-243.

12. Morita K, Furuse M, Fujimoto K, Tsukita S. Claudin multigene family encoding four-transmembrane domain protein components of tight junction strands. Proc. Natl. Acad. Sci. U S A. 1999; 96:511–516. [PubMed: 9892664]

13. Furuse M, Fujita K, Hiiragi T, Fujimoto K, Tsukita S. Claudin-1 and -2: novel integral membrane proteins localizing at tight junctions with no sequence similarity to occludin. J. Cell Biol. 1998; 141:1539–1550. [PubMed: 9647647]

14. Roy A, Ganesh G, Sippola H, Bolin S, Sawesi O, Dagalv A, Schlenner SM, Feyerabend T, Rodewald HR, Kjellen L, Hellman L, Abrink M. Mast Cell Chymase Degrades the Alarmins Heat Shock Protein 70, Biglycan, HMGB1, and Interleukin-33 (IL-33) and Limits Danger-induced Inflammation. J Biol. Chem. 2014; 289:237–250. [PubMed: 24257755]

15. Murphy GF, Austen KF, Fonferko E, Sheffer AL. Morphologically distinctive forms of cutaneous mast cell degranulation induced by cold and mechanical stimuli: an ultrastructural study. J. Allergy Clin. Immunol. 1987; 80:603–611. [PubMed: 3668125]

16. Weiser MR, Williams JP, Moore FD Jr, Kobzik L, Ma M, Hechtman HB, Carroll MC. Reperfusion injury of ischemic skeletal muscle is mediated by natural antibody and complement. J. Exp. Med. 1996; 183:2343–2348. [PubMed: 8642343]

17. Arizono N, Matsuda S, Hattori T, Kojima Y, Maeda T, Galli SJ. Anatomical variation in mast cell nerve associations in the rat small intestine, heart, lung, and skin. Similarities of distances between neural processes and mast cells, eosinophils, or plasma cells in the jejunal lamina propria. Lab.. Investig. 1990; 62:626–634. [PubMed: 2342332]

18. Groschwitz RK, Hogan SP. Intestinal barrier function: molecular regulation and disease pathogenesis. J. Allergy Clin. Immunol. 2009; 124:3–20. [PubMed: 19560575]

19. De Benedetto A, Kubo A, Beck LA. Skin barrier disruption: a requirement for allergen sensitization? J. Invest. Dermatol. 2012; 132:949–963. [PubMed: 22217737]

20. De Benedetto A, Rafaels NM, McGirt LY, Ivanov AI, Georas SN, Cheadle C, Berger AE, Zhang K, Vidyasagar S, Yoshida T, Boguniewicz M, Hata T, Schneider LC, Hanifin JM, Gallo RL, Novak N, Weidinger S, Beaty TH, Leung DY, Barnes KC, Beck LA. Tight junction defects in patients with atopic dermatitis. J. Allergy Clin. Immunol. 2011; 127:773–786. e771–e777. [PubMed: 21163515]

21. Kirschner N, Poetzl C, von den Driesch P, Wladykowski E, Moll I, Behne MJ, Brandner JM. Alteration of tight junction proteins is an early event in psoriasis: putative involvement of proinflammatory cytokines. Am. J. Pathol. 2009; 175:1095–1106. [PubMed: 19661441]

22. Groschwitz KR, Ahrens R, Osterfeld H, Gurish MF, Han X, Abrink M, Finkelman FD, Pejler G, Hogan SP. Mast cells regulate homeostatic intestinal epithelial migration and barrier function by a chymase/Mcpt4-dependent mechanism. Proc. Natl. Acad. Sci. U S A. 2009; 106:22381–22386. [PubMed: 20018751]

23. Tchougounova E, Lundequist A, Fajardo I, Winberg JO, Abrink M, Pejler G. A key role for mast cell chymase in the activation of pro-matrix metalloprotease-9 and pro-matrix metalloprotease-2. J. Biol. Chem. 2005; 280:9291–9296. [PubMed: 15615702]

24. Ghildyal N, Friend DS, Stevens RL, Austen KF, Huang C, Penrose JF, Sali A, Gurish MF. Fate of two mast cell tryptases in V3 mastocytosis and normal BALB/c mice undergoing passive systemic anaphylaxis: prolonged retention of exocytosed mMCP-6 in connective tissues, and rapid accumulation of enzymatically active mMCP-7 in the blood. J. Exp. Med. 1996; 184:1061–1073. [PubMed: 9064323]

25. Humphries DE, Wong GW, Friend DS, Gurish MF, Qiu WT, Huang C, Sharpe AH, Stevens RL. Heparin is essential for the storage of specific granule proteases in mast cells. Nature. 1999; 400:769–772. [PubMed: 10466726]

26. Serafin WE, Katz HR, Austen KF, Stevens RL. Complexes of heparin proteoglycans, chondroitin sulfate E proteoglycans, and [3H]diisopropyl fluorophosphate-binding proteins are exocytosed from activated mouse bone marrow-derived mast cells. J. Biol. Chem. 1986; 261:15017–15021. [PubMed: 3095324]

27. Karlson U, Pejler G, Froman G, Hellman L. Rat mast cell protease 4 is a beta-chymase with unusually stringent substrate recognition profile. J. Biol. Chem. 2002; 277:18579–18585. [PubMed: 11896050]

28. Pejler G, Sadler JE. Mechanism by which heparin proteoglycan modulates mast cell chymase activity. Biochemistry. 1999; 38:12187–12195. [PubMed: 10508424]

29. Wintroub BU, Mihm MC Jr, Goetzl EJ, Soter NA, Austen KF. Morphologic and functional evidence for release of mast-cell products in bullous pemphigoid. N. Engl. J. Med. 1978; 298:417–421. [PubMed: 340950]

30. Lin L, Bankaitis E, Heimbach L, Li N, Abrink M, Pejler G, An L, Diaz LA, Werb Z, Liu Z. Dual targets for mouse mast cell protease-4 in mediating tissue damage in experimental bullous pemphigoid. J. Biol. Chem. 2011; 286:37358–37367. [PubMed: 21880713]

Abbreviations used in this article

MC	mast cell
CAE	chloroacetate esterase reactivity
EM	electron microscopy
LPF	low-power field
mMCP	mouse MC protease
PBS	phosphate buffered saline
PMN	neutrophil
TJ	tight junction
UA	unit area
WT	wild type

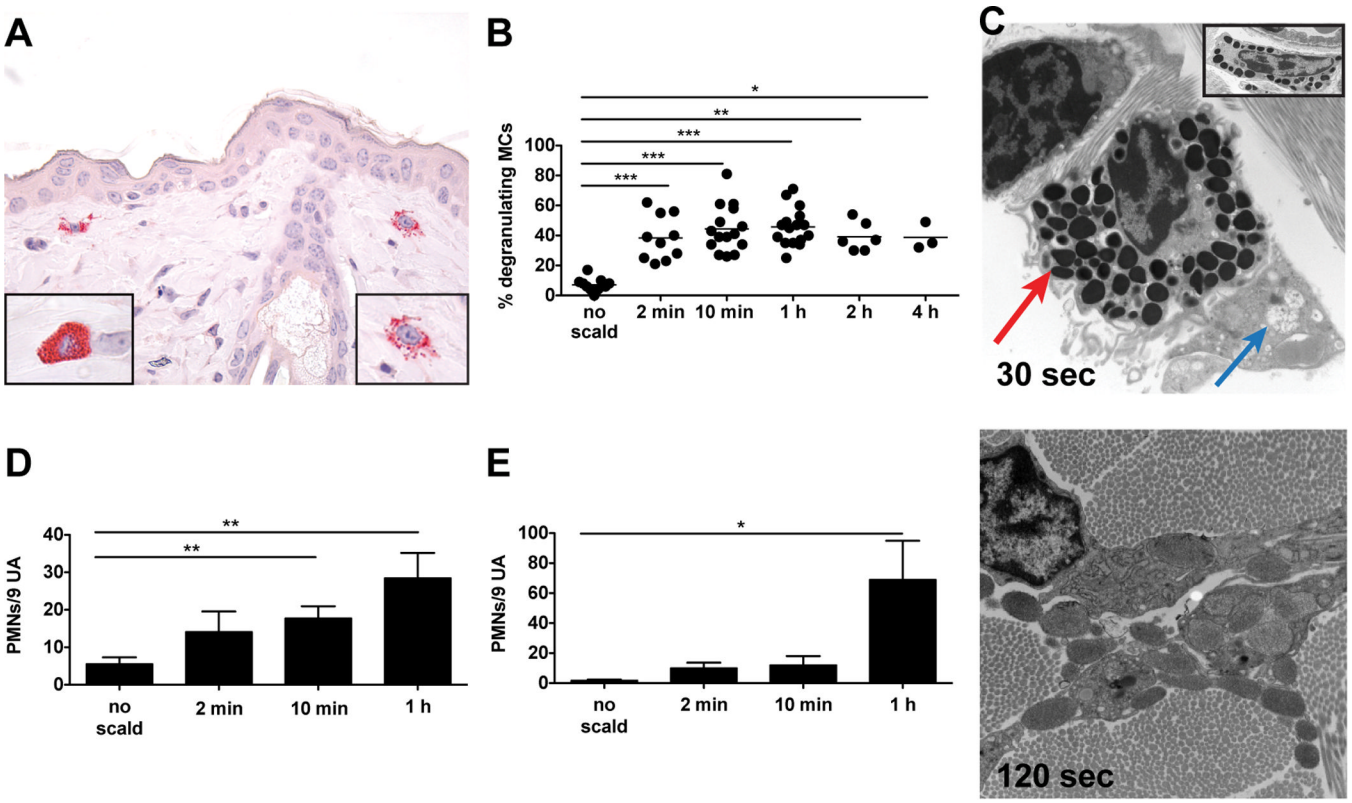

FIGURE 1.

MC degranulation is an immediate response to thermal challenge in WT mice. **(A)** Light micrograph of degranulating MCs in the skin as detected by CAE reactivity, 1 h after scald (magnification 630×). Left hand insert shows an intact MC, right hand insert shows a degranulating MC. **(B)** MC degranulation was quantitated in the skin at various times after the thermal challenge. The graph presents the percent of total MCs with >3 extracellular granules. Each dot is a separate mouse and the bar indicates mean value from 7 experiments. **(C)** EM of a degranulating MC captured 30 s and 120 s after thermal injury (original magnification 8,000×). At 30 s (*top panel*), there is segmental degranulation (*blue arrow*) and granules typical of a resting MC (*red arrow*). At 120 s (*bottom panel*), there is extensive MC degranulation (original magnification 12,000×). The top panel insert shows a fully granulated (intact) MC (original magnification 8,000×). **(D, E)** Quantitation of PMNs marginating (D) and extravasated (E) at various time points after thermal trauma. Data represent mean ± SEM, n=8–11 per time point from 7 experiments. *$p < 0.05$, **$p < 0.01$, ***$p < 0.001$.

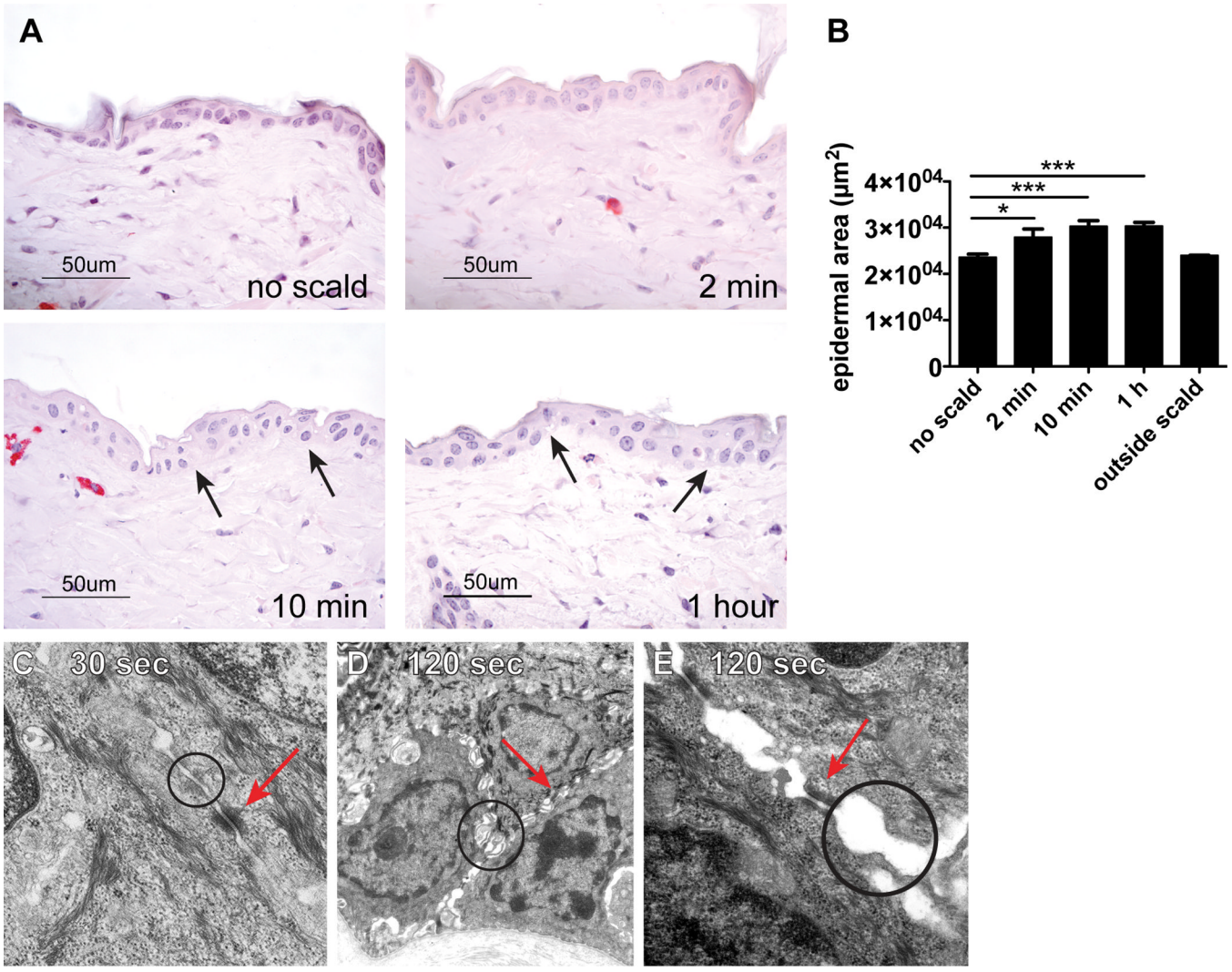

FIGURE 2.

Disruption of TJs is an immediate epidermal response to thermal injury in WT mice. **(A)** The histology of normal WT mouse epidermis after shaving without thermal injury and at 2 min, 10 min, and 1 h after thermal trauma showing epidermal edema. Spongiosis is notable at 10 min and 1 h (*arrows*). **(B)** Epidermal area of unscalded skin and of skin after thermal injury at time points indicated and of uninjured skin from a dorsal area distant from the scalded area 1 h after injury (outside scald) (mean ± SEM, n=7–12 mice per time point from 5 experiments, outside scald n=2, *$p<0.05$, ***$p<0.001$). **(C)** By EM at 30 s, the epidermis is ultrastructurally unremarkable with normally spaced plasma membranes (TJs *circle*) and unaltered desmosomes (*arrow*) (original magnification is 20,000×). **(D, E)** The ultrastructure of the epidermis at 120 s after thermal injury shows variable condensation of tonofilaments and widening of intercellular spaces accompanied by formation of microvilli and apparent disruption of TJs (*circles*) while desmosomes (*arrows*) remained intact; original magnification 10,000× (D) and 50,000× (E).

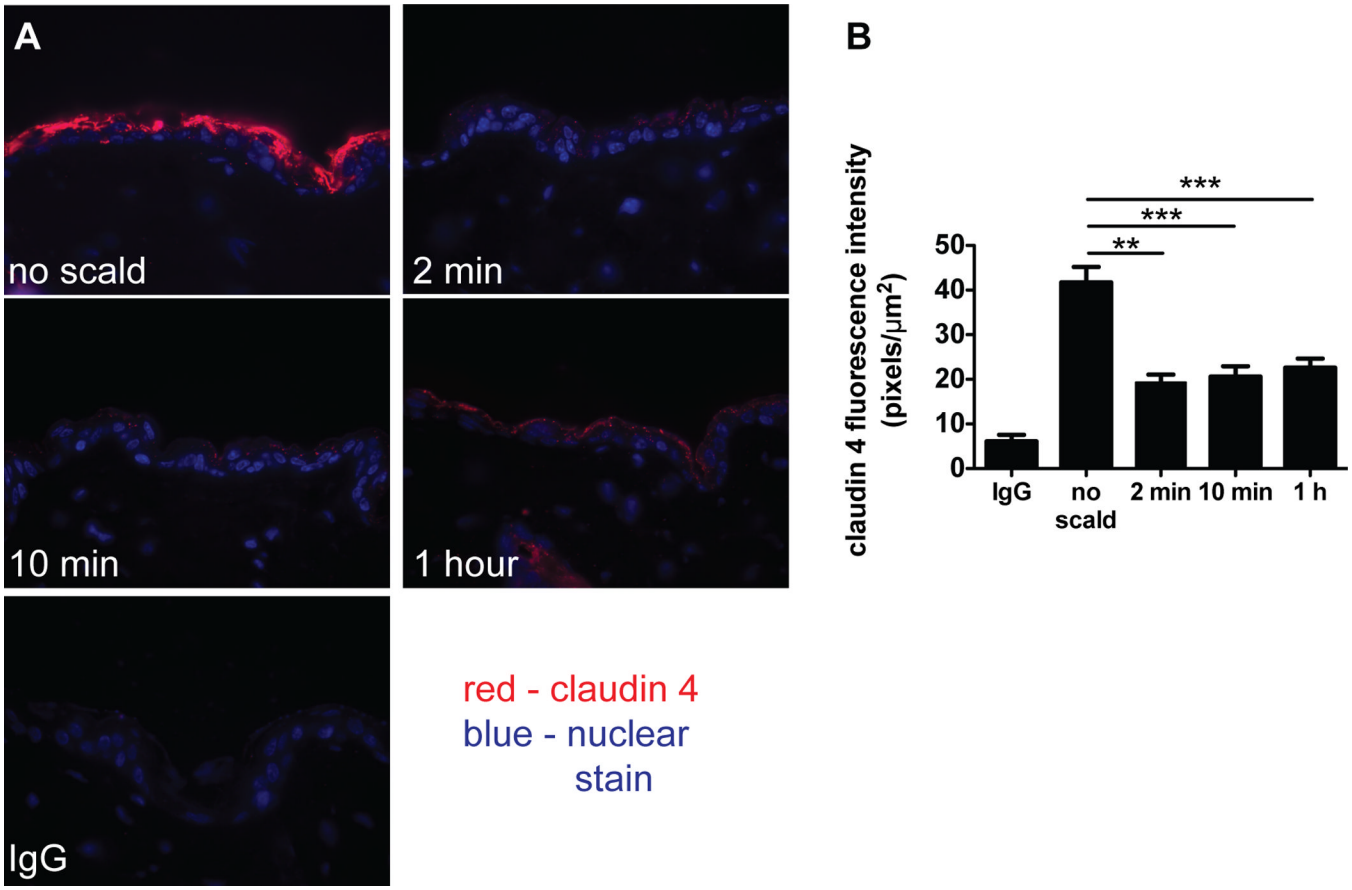

FIGURE 3.

Immunodetection of the TJ protein claudin 4 diminishes after thermal injury. **(A)** Immunodetection of claudin 4 in uninjured skin and at various time points after thermal injury (magnification 600×). **(B)** Quantitation of claudin 4 in the epidermis demonstrating decreased fluorescence intensity after the injury. Data represent mean ± SEM, n=6–12 mice per time point from 4 experiments, ** $p<0.01$, *** $p<0.001$

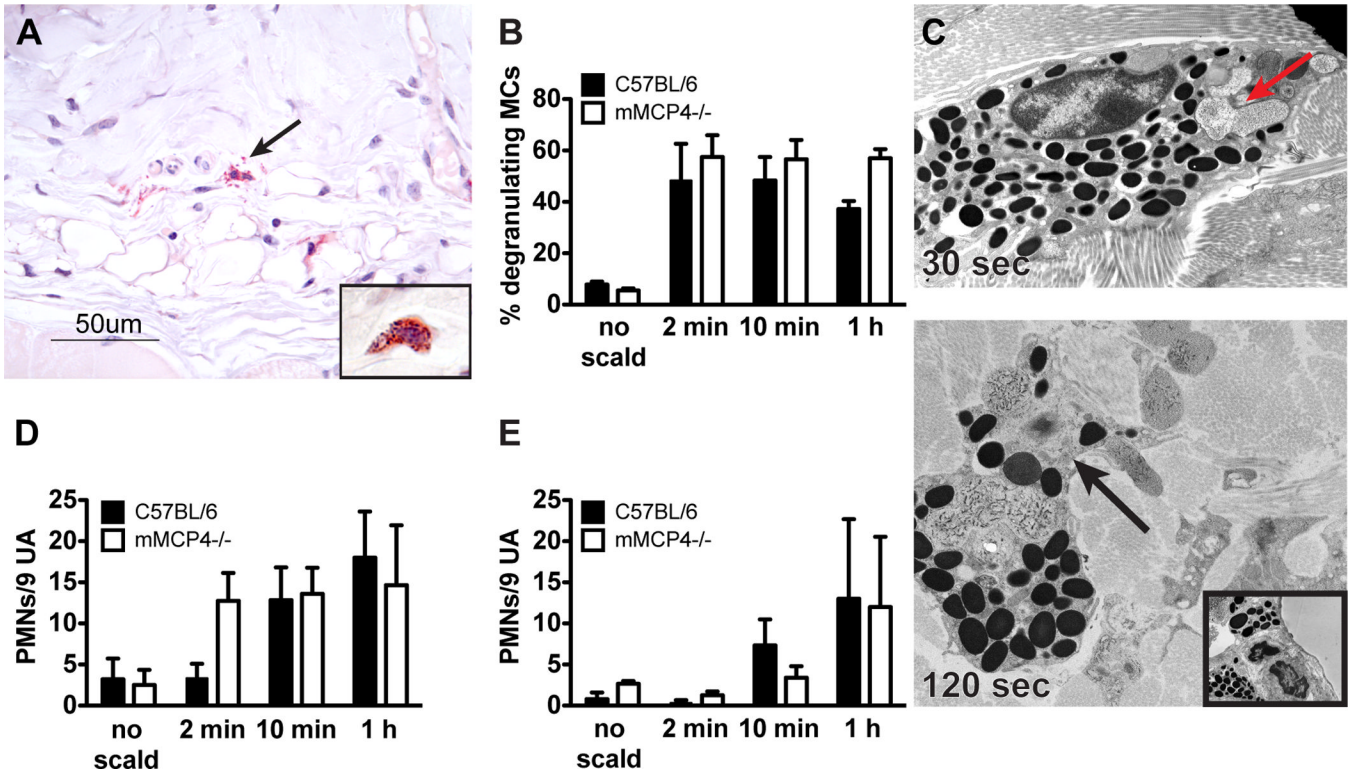

FIGURE 4.

MC degranulation after thermal challenge is preserved in mMCP4$^{-/-}$ mice. **(A)** Histological demonstration (CAE reactivity) of degranulating MCs in the skin of an mMCP4$^{-/-}$ mouse after thermal challenge (*arrow* indicates extruded granules). Insert shows an intact MC from mMCP4$^{-/-}$ unscalded skin. **(B)** MC degranulation in mMCP4$^{-/-}$ mice is similar to that observed in WT mice. **(C)** EM of a mMCP4$^{-/-}$ MC captured 30 s after scald injury demonstrating zonal MC degranulation (*arrow*, *top panel*, original magnification 10,000×). By 120 s, prominent zonal MC degranulation is present (*arrow*, *bottom panel*, original magnification 10,000×). Insert shows an intact MC from mMCP4$^{-/-}$ unscalded skin (original magnification 8000×). **(D, E)** PMN margination (D) and tissue influx (E) in mMCP4$^{-/-}$ mice is comparable to WT controls. Data represent mean ± SEM, n=3–6 mice per time point from 3 experiments.

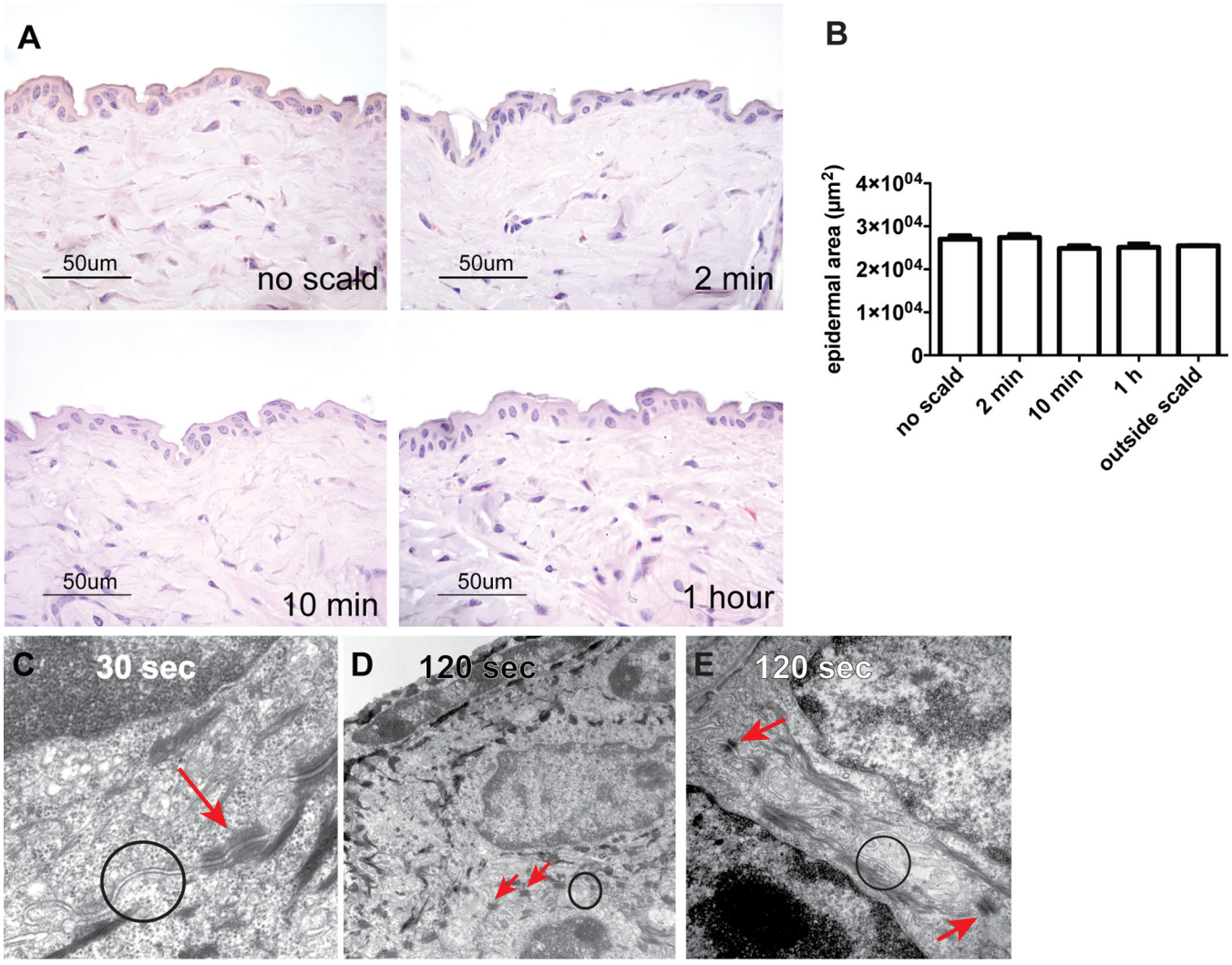

FIGURE 5.

Thermal injury in mMCP4$^{-/-}$ mice does not lead to epidermal changes. **(A, B)** The histology of the epidermis in mMCP4$^{-/-}$ mice after shaving without thermal injury and at 2 min, 10 min, and 1 h after thermal trauma showing no change in epidermal thickness. **(B)** Epidermal area of unscalded skin and of skin after thermal challenge at time points indicated and of uninjured skin from a dorsal area distant from the scalded area 1 h after injury (outside scald). Data represent means ± SEM, n=3–7 mice per time point from 3 experiments"outside scald" n=2. **(C–E)** EM of mMCP4$^{-/-}$ skin 30 and 120 s after scald injury. At 30 s (C) the plasma membranes are normally spaced with intact TJs (*circle*) and desmosomes (*arrow*) (original magnification 50,000×). At 120 s (D magnification 15,000×, E magnification 30,000×), the epidermis remains ultrastructurally unaltered with normally spaced plasma membranes with intact TJs (*circles*), and desmosomes (*arrows*).

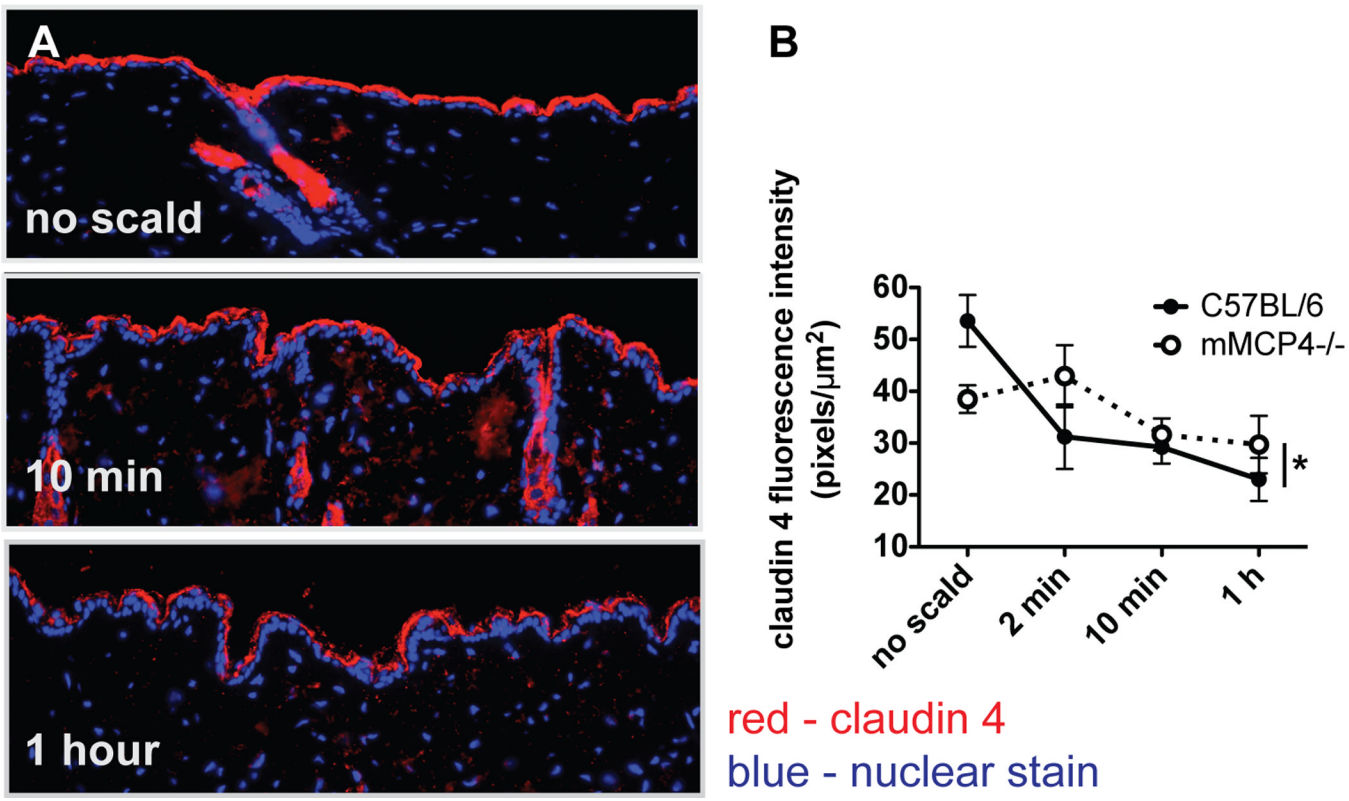

FIGURE 6.

Immunodetection of claudin 4 in mMCP4$^{-/-}$ mice after thermal challenge is not significantly altered. **(A)** Immunofluorescence detection of claudin 4 at baseline, 10 min, and 1 h after scald injury of mMCP4$^{-/-}$ mice (magnification 200×). **(B)** Quantitation of claudin 4 in the epidermis of mMCP4$^{-/-}$ and of WT mice after thermal injury at various time points as indicated. Compared to WT, there is no significant decrement in the level of claudin 4 in mMCP4$^{-/-}$ mice. Data represent mean ± SEM, n=3–8 mice per time point from 3 experiments. *Strains are significantly different by 2-way ANOVA analysis.

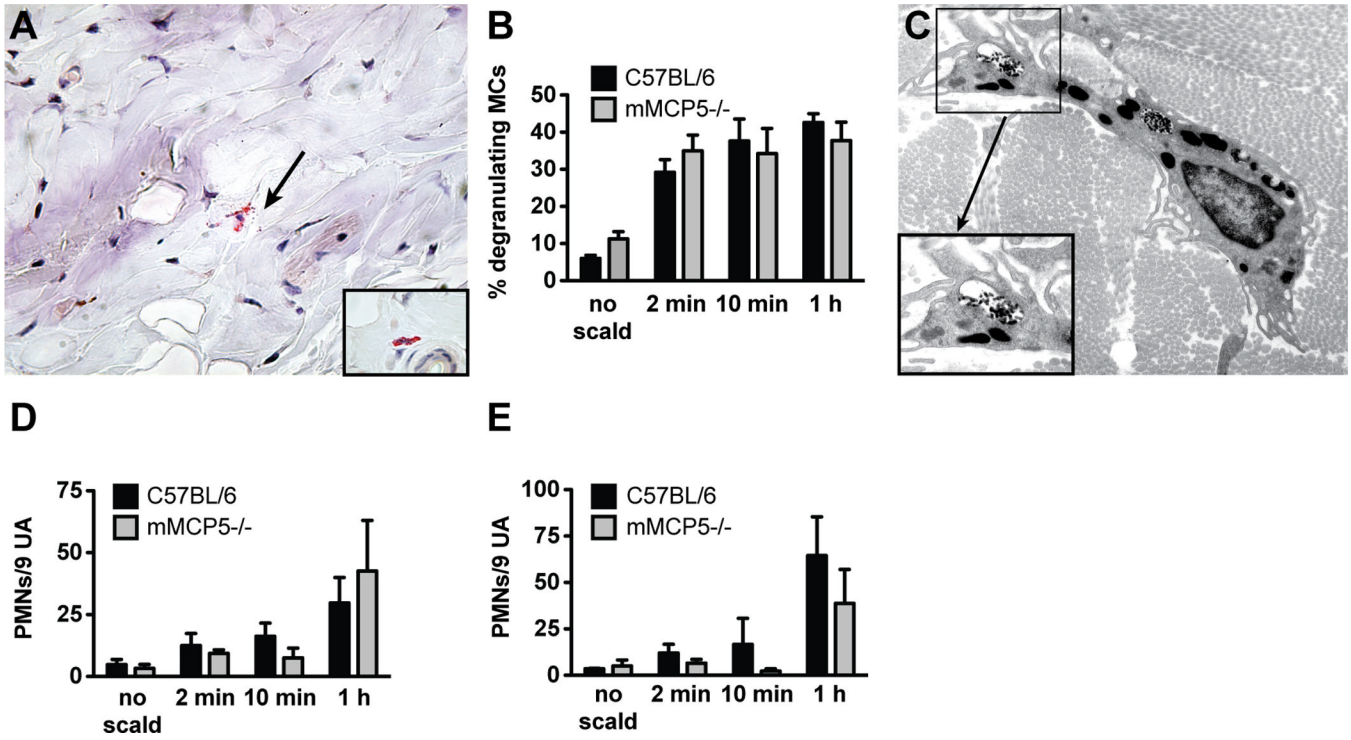

FIGURE 7.

MC degranulation after thermal challenge is preserved in mMCP5$^{-/-}$ mice. **(A)** Histological demonstration (CAE reactivity) of degranulating MCs in the skin of an mMCP5$^{-/-}$ mouse (*arrow* indicates extruded granules). Insert shows an intact MC from mMCP5$^{-/-}$ mouse skin (magnification 630×). **(B)** MC degranulation in mMCP5$^{-/-}$ mice shows similar percentage to that observed in WT mice (mean ± SEM, n=4–5 mice per time point from 2 experiments). **(C)** EM of a mMCP5$^{-/-}$ MC captured 120 s after scald injury (magnification 12,000×) demonstrating zonal MC degranulation (box). Insert shows higher magnification of degranulation (magnification 30,000×). **(D, E)** PMN margination (D) and tissue influx (E) in thermally challenged skin of mMCP5$^{-/-}$ and WT mice (mean ± SEM, n=4–7 mice per time point from 3 experiments).

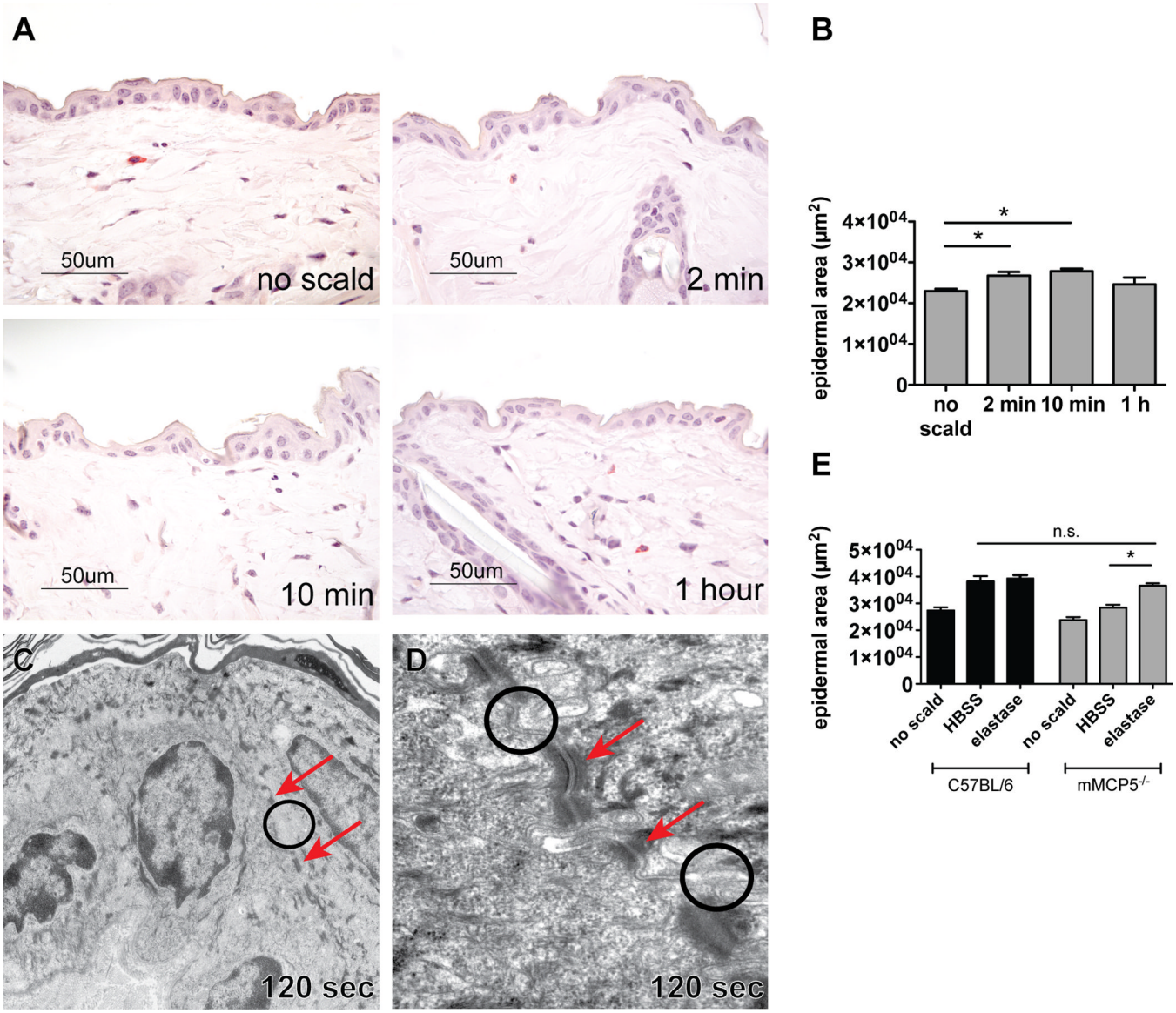

FIGURE 8.

Thermal challenge of mMCP5$^{-/-}$ mice leads to mild epidermal changes. **(A)** Histology of normal mMCP5$^{-/-}$ mouse skin after shaving, no thermal injury and of thermally challenged mMCP5$^{-/-}$ skin 2 min, 10 min and 1 h after injury. **(B)** Epidermal area of unscalded and scalded skin measured 2 min, 10 min, and 1 h after thermal challenge of mMCP5$^{-/-}$ mice (mean ± SEM n=4–6 mice per time point from 3 experiments). **(C)** EM of mMCP5$^{-/-}$ mouse epidermis 120 s after thermal challenge showing normal appearance with intact TJs (*circle*) and desmosomes (*arrows*) (magnification 10,000×). **(D)** Higher magnification (60,000×) showing intact TJs (*circles*) and desmosomes (*arrows*) after thermal challenge. **(E)** Epidermal area in WT mice (black bars) and mMCP5$^{-/-}$ mice (grey bars) after application of HBSS or elastase to the scald area immediately after scalding, (mean ± SEM, n=3–5 mice per group from 2 separate experiments, mMCP5$^{-/-}$ no scald and WT elastase groups n=2)

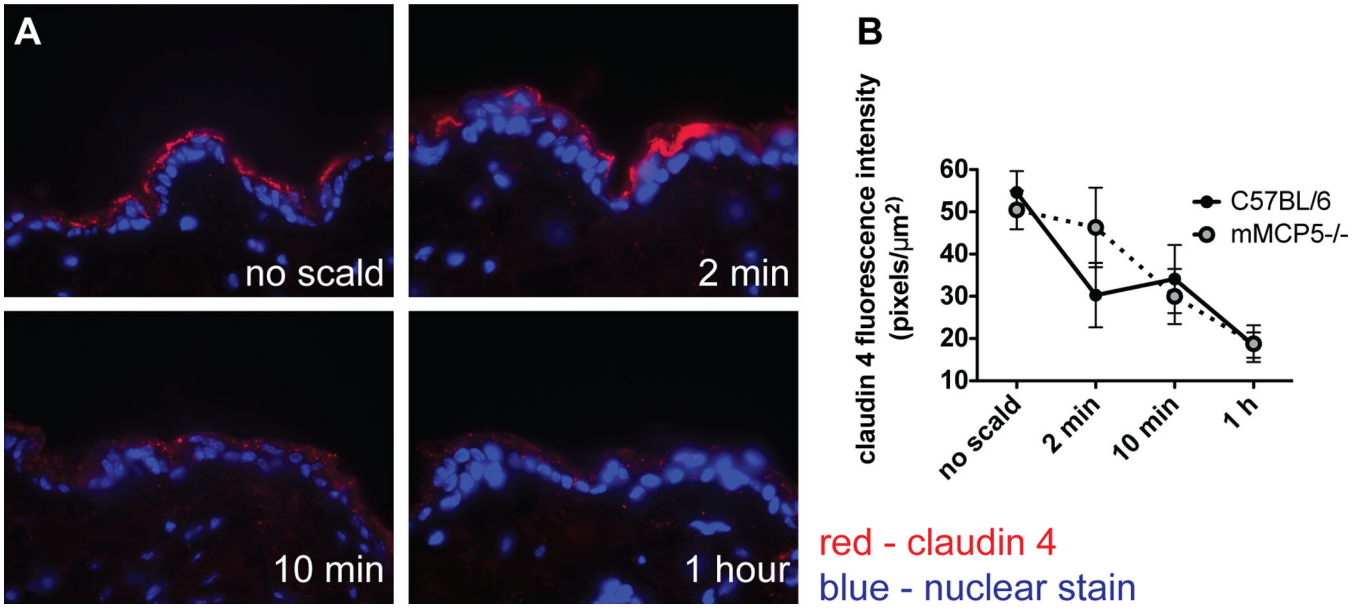

FIGURE 9.

Immunodetection of claudin 4 in mMCP5$^{-/-}$ mice diminishes after thermal trauma. **(A)** Immunofluorescence detection of claudin 4 expression in mMCP5$^{-/-}$ mouse skin after thermal challenge at indicated time points (magnification 600×). **(B)** Quantitation of claudin 4 fluorescence in the epidermis of WT and mMCP5$^{-/-}$ mice shows depletion in both strains (mean ± SEM, n=4–6 mice per time point from 3 experiments).